

A THEORY OF FLUORESCENCE POLARIZATION DECAY IN MEMBRANES

KAZUHIKO KINOSITA, JR., SUGURU KAWATO, AND AKIRA IKEGAMI,
*Department of Physics, Faculty of Science, University of Tokyo,
Bunkyo-ku, Tokyo 113, Japan*

ABSTRACT Decay of fluorescence polarization after an impulsive excitation is correlated with wobbling motion of fluorescent molecules in membranes. The motion is characterized by two parameters, a "wobbling diffusion constant" and a "degree of orientational constraint" both of which can be determined directly from experimentally obtained decay. Detailed discussion, including theoretically calculated time-courses of polarization decay, is given for several types of molecules embedded in lipid bilayers; these types cover a large part of fluorescent probes available at present. The theory is useful for the analysis of fluorescence polarization decay in any system where the orientation of fluorophore is restricted by the surrounding structure.

INTRODUCTION

The so-called nanosecond fluorescence polarization technique has enabled us to follow the rotational motion of molecules in the nanosecond range (1-3). Unlike classical polarization studies using steady-state excitation, this time-dependent measurement readily resolves complex motions such as rotation of asymmetric or flexible molecules in solution (1,4). Although most applications of this technique have concerned the size or the conformation of macromolecules in solution, its potential usefulness lies in the determination of the dynamic structure of higher systems, e.g. biomembranes.

In membranes, several nanosecond experiments to date (5-8) indicate a general pattern: when fluorescent molecules embedded in membranes are excited by a pulse of polarized light, the polarization of emitted fluorescence is maximal at the moment of excitation and decays to a stationary value after a certain period of time. This pattern suggests that molecules in membranes exhibit wobbling motions rather than free rotation. The rate of the polarization decay reflects the frequency of fluctuation of molecular orientation in the membrane, while the stationary value reflects the orientational constraint imposed by neighboring molecules. Thus we can infer the dynamics of molecular interactions, essential for the understanding of structure and function of biological membranes.

This article describes a theory that allows a quantitative interpretation of polariza-

Dr. Kinoshita's present address is: Department of Physiological Chemistry, The Johns Hopkins University School of Medicine, Baltimore, Md. 21205. Correspondence should be addressed to Dr. Ikegami.

tion decay in membrane in terms of a "wobbling diffusion constant" and a "degree of orientational constraint." The theory deals with suspensions of membranes (intact or ghost cells, liposomes, etc.), because precise measurements can readily be made on macroscopic suspensions (7). The primary system considered is that of lipid bilayers containing fluorescent molecules which may be lipid analogues or (labeled) membrane proteins.

The description of the theory begins with the introduction of a general formalism in which fluorescence anisotropy, a measure of the degree of polarization, is correlated with an evolution function that describes the rotational motion of the fluorescent molecules. Then the formalism is adapted to membrane suspension, considered to be equivalent to an ensemble of planar membrane segments. The wobbling diffusion constant and the degree of orientational constraint characterize the evolution function defined within each segment. Finally, simple but well-defined models are presented to describe several possible modes of wobbling motion in membranes; interpretation of experimental data is straightforward and clear-cut when one of these models applies. An example of application, the dynamic structure of lipid bilayers, is analyzed by the theory. The concluding section describes the broad applicability of this theory.

FLUORESCENCE ANISOTROPY OF A SYSTEM ISOTROPIC AS A WHOLE

The system we consider in this article is a suspension of membranes that contain fluorescent molecules. A distinct feature of such a system is that it is isotropic as a whole. In other words, the rotation of the whole system in space does not affect the result of an observation. In this section, we develop a formal theory of fluorescence anisotropy applicable to any such isotropic system.

First we adopt the following convention: a letter printed in boldface type denotes a unit vector, with which we specify a direction in space; an integration such as $\int d\mu$ represents $\int \sin \alpha d\alpha d\beta$ where α and β are the polar and azimuthal angles of μ with respect to some fixed direction.

Taking mutually orthogonal unit vectors, ξ , η , ϵ in space (see Fig. 1), we excite a sample with a pulsed light polarized in the direction of ϵ . Fluorescence intensity components polarized in ξ - and ϵ -directions, $I_\xi(t)$ and $I_\epsilon(t)$, are observed in the direction of η as functions of time t after the excitation. We define the fluorescence anisotropy $r(t)$ by

$$r(t) = [I_\epsilon(t) - I_\xi(t)]/[I_\epsilon(t) + 2I_\xi(t)]. \quad (1)$$

Now we consider a fluorescent molecule in the sample. Let μ_a and μ_e be the directions of the transition moment corresponding to the absorption of the excitation light and the emission of fluorescence, respectively. We assume a monochromatic excitation, whereupon μ_a and μ_e are definite directions in the molecule and make a fixed angle λ . Note that the set $\{\mu_a, \mu_e\}$ completely defines the orientation of the molecule in space (the case $\lambda = 0$ can be included as a limit).

The molecule above, if in its excited state, contributes to the fluorescence intensity

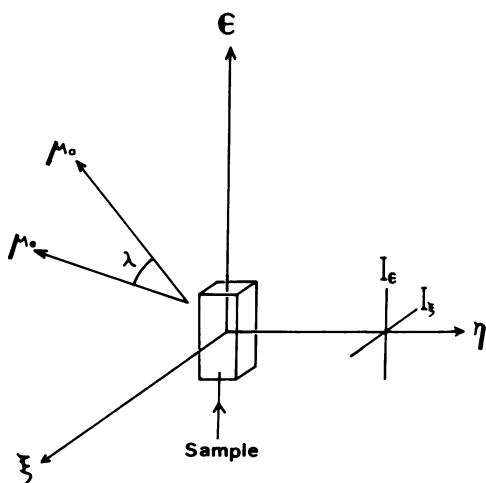


FIGURE 1 Geometry of the system. Excitation light is polarized in the direction of ϵ . Fluorescence is observed along η . The two vectors μ_a and μ_e represent the directions of absorption and emission transition moments of a fluorophore in the sample.

component I_ϵ in proportion to $(\epsilon \cdot \mu_e)^2$. Thus

$$I_\epsilon(t) = K(t) \langle (\epsilon \cdot \mu_e)^2 \rangle_t, \quad (2)$$

where $K(t) \propto \exp(-t/\tau)$ represents the decay of the number of molecules in the excited state, τ being the lifetime, and $\langle \rangle_t$ denotes the average over all the excited state molecules. Similarly,

$$I_\xi(t) = K(t) \langle (\xi \cdot \mu_e)^2 \rangle_t, \quad I_\eta(t) = K(t) \langle (\eta \cdot \mu_e)^2 \rangle_t. \quad (3)$$

For our isotropic sample, symmetry requires the following relation:

$$I_\xi(t) = I_\eta(t) = \frac{1}{2}K(t) \langle 1 - (\epsilon \cdot \mu_e)^2 \rangle_t. \quad (4)$$

Substituting Eqs. 2 and 4 into Eq. 1, we obtain

$$r(t) = \langle \frac{1}{2}[3(\epsilon \cdot \mu_e)^2 - 1] \rangle_t \equiv \langle P_2(\epsilon \cdot \mu_e) \rangle_t, \quad (5)$$

where P_2 is the Legendre polynomial of order 2.

To calculate the average in Eq. 5, let us introduce a distribution function $W(\mu_a, \mu_e, t)$, the probability that we would find a molecule with orientation $\{\mu_a, \mu_e\}$ in the sample at time t regardless of whether it is in the excited state. The function W is normalized such that

$$\int W(\mu_a, \mu_e, t) d\mu_a d\mu_e = 1. \quad (6)$$

For the evolution of W with time, we define $G(\mu'_a, \mu'_e, t' | \mu_a, \mu_e, t)$ as the probability that a molecule with orientation $\{\mu'_a, \mu'_e\}$ at time t' will rotate into a new orientation $\{\mu_a, \mu_e\}$ by time t . Thus,

$$W(\mu_a, \mu_e, t) = \iint W(\mu'_a, \mu'_e, t') G(\mu'_a, \mu'_e, t' | \mu_a, \mu_e, t) d\mu'_a d\mu'_e. \quad (7)$$

Here we understand that both W and G contain a factor $\delta(\mu_a \cdot \mu_e - \cos \lambda)$ which assures the fixed angle between the two moments. For the isotropic sample, stationary distribution W^s is given by

$$W^s(\mu_a, \mu_e) = (1/8 \pi^2) \delta(\mu_a \cdot \mu_e - \cos \lambda). \quad (8)$$

Now Eq. 5 can be rewritten as follows:

$$r(t) = \iiint P_2(\epsilon \cdot \mu_e) 3(\epsilon \cdot \mu'_a)^2 W^s(\mu'_a, \mu'_e) G(\mu'_a, \mu'_e, 0 | \mu_a, \mu_e, t) d\mu'_a d\mu'_e d\mu_a d\mu_e. \quad (9)$$

Here, at time 0, the polarized excitation light selectively excites the molecules in stationary distribution W^s in proportion to $3(\epsilon \cdot \mu'_a)^2$, where the factor 3 assures a unit excitation; the product $3(\epsilon \cdot \mu'_a)^2 W^s G$, upon integration with respect to μ'_a and μ'_e , yields the probability that a molecule in the excited state has the orientation $\{\mu_a, \mu_e\}$ at time t .

Because of the isotropic nature of the sample, $r(t)$ does not depend on the direction of ϵ in space. Therefore, we can replace the right-hand side of Eq. 9 by the average over ϵ :

$$r(t) = \frac{1}{4\pi} \iiint P_2(\epsilon \cdot \mu_e) 3(\epsilon \cdot \mu'_a)^2 W^s(\mu'_a, \mu'_e) G(\mu'_a, \mu'_e, 0 | \mu_a, \mu_e, t) d\mu'_a d\mu'_e d\mu_a d\mu_e d\epsilon. \quad (10)$$

We first perform the integration with ϵ , making use of the addition theorem:

$$P_2(\epsilon \cdot \mu_e) = P_2(\epsilon \cdot \mu'_a) P_2(\mu'_a \cdot \mu_e) + \frac{1}{3} P_2^1(\epsilon \cdot \mu'_a) P_2^1(\mu'_a \cdot \mu_e) \cos(\phi - \phi') + \frac{1}{12} P_2^2(\epsilon \cdot \mu'_a) P_2^2(\mu'_a \cdot \mu_e) \cos 2(\phi - \phi'), \quad (11)$$

where P_2^1 and P_2^2 are the associated Legendre polynomials and ϕ and ϕ' are the azimuthal angles of ϵ and μ_e around μ'_a . The second and third terms in Eq. 11 drop on integration with ϕ , leaving

$$r(t) = 0.4 \iiint P_2(\mu'_a \cdot \mu_e) W^s(\mu'_a, \mu'_e) G(\mu'_a, \mu'_e, 0 | \mu_a, \mu_e, t) d\mu'_a d\mu'_e d\mu_a d\mu_e. \quad (12)$$

Thus the fluorescence anisotropy $r(t)$ is determined by the evolution function G of the sample. In particular, G reduces to $\delta(\mu_a - \mu'_a) \delta(\mu_e - \mu'_e)$ for $t = 0$. Hence the substitution of Eq. 8 into 12 leads to the familiar expression of the limiting anisotropy r_0 :

$$r_0 \equiv r(0) = 0.4 P_2(\cos \lambda). \quad (13)$$

In the following sections, we often refer to the special cases: (a) μ_a and μ_e are approximately parallel, i.e. $\lambda \cong 0$, $r_0 \cong 0.4$; (b) $W(\mu_a, \mu_e, t)$ is independent of μ_a , i.e. the probability of a particular orientation depends only on μ_e . Case *b* applies when the fluorescent molecule under consideration is axially symmetric around μ_e . In both these cases, Eq. 12 is further rewritten as follows. We again expand $P_2(\mu'_a \cdot \mu_e)$ as

$$P_2(\mu'_a \cdot \mu_e) = P_2(\mu'_a \cdot \mu'_e) P_2(\mu'_e \cdot \mu_e) + \frac{1}{3} P_2^1(\mu'_a \cdot \mu'_e) P_2^1(\mu'_e \cdot \mu_e) \cos(\psi - \psi') + \frac{1}{12} P_2^2(\mu'_a \cdot \mu'_e) P_2^2(\mu'_e \cdot \mu_e) \cos 2(\psi - \psi'), \quad (14)$$

where ψ and ψ' are the azimuthal angles of μ'_a and μ_e around μ'_e . In case *a* the second and the third terms in Eq. 14 are clearly negligible. In case *b*, these terms vanish on integration with respect to ψ , because $\int G(\mu'_a, \mu'_e, 0 | \mu_a, \mu_e, t) d\mu_a$ in Eq. 12 does not depend on ψ . For both cases, therefore, we obtain

$$r(t) = r_0 \iint P_2(\mu'_e \cdot \mu_e) \hat{W}^s(\mu'_e) \hat{G}(\mu'_e, 0 | \mu_e, t) d\mu'_e d\mu_e, \quad (15)$$

where

$$\hat{W}^s(\mu'_e) \equiv \int W^s(\mu'_a, \mu'_e) d\mu'_a, \quad (16)$$

$$\hat{G}(\mu'_e, 0 | \mu_e, t) \equiv W^s(\mu'_e)^{-1} \int W^s(\mu'_a, \mu'_e) G(\mu'_a, \mu'_e, 0 | \mu_a, \mu_e, t) d\mu'_a d\mu_a. \quad (17)$$

This expression is particularly useful for case *b*, because \hat{G} may be regarded as the evolution function for $\hat{W}(\mu_e, t)$:

$$\hat{W}(\mu_e, t) \equiv \int W(\mu_a, \mu_e, t) d\mu_a = \int \hat{W}(\mu'_e, t') \hat{G}(\mu'_e, t' | \mu_e, t) d\mu'_e. \quad (18)$$

FLUORESCENCE ANISOTROPY OF A MEMBRANE SUSPENSION

It has been shown in the preceding section that the evolution function $G(\mu'_a, \mu'_e, t' | \mu_a, \mu_e, t)$ completely determines the fluorescence anisotropy $r(t)$ of an isotropic sample. If the distribution function $W(\mu_a, \mu_e, t)$ satisfies a suitable differential equation, G can be obtained as the Green function of the equation. This is the case for fluorescent molecules suspended in an isotropic medium, where W is governed by a simple diffusion equation. The corresponding expression for $r(t)$, for the most general case of the completely asymmetric molecule, has been given by Tao (9), whose results actually are confined to cases *a* and *b* above, and by Belford et al. (10).

When fluorescent molecules are embedded in membranes, however, the probability of reorientation $\{\mu'_a, \mu'_e\} \rightarrow \{\mu_a, \mu_e\}$ for a particular molecule depends on the orientation of the membrane in which the molecule is placed. Hence the distribution function $W(\mu_a, \mu_e, t)$ defined over the whole sample no longer satisfies a simple differential equation. In this section, therefore, we correlate $r(t)$ with a distribution function defined within a particular segment of membrane in which the motion of the fluorescent molecules can be described by a well-defined differential equation.

We suppose that a suspension of membrane is equivalent to an ensemble of planar membrane segments. Within a segment designated by its normal \mathbf{n} , we define the distribution function of the orientation of the fluorescent molecules $w_{\mathbf{n}}(\mu_a, \mu_e, t)$ as well as its evolution function $g_{\mathbf{n}}(\mu'_a, \mu'_e, t' | \mu_a, \mu_e, t)$ and the stationary distribution $w_{\mathbf{n}}^s(\mu_a, \mu_e)$. These functions satisfy equations analogous to Eqs. 6 and 7. Note, however, that the environment of the molecules is not isotropic in the membrane segment, so that $w_{\mathbf{n}}^s$ is no longer given by Eq. 8. Corresponding quantities with circumflexes are defined as in Eqs. 16–18.

Now the product $W^s G$ in Eq. 12 can be replaced with the average of $w_{\mathbf{n}}^s g_{\mathbf{n}}$ over \mathbf{n} :

$$r(t) = (1/N) \sum_{\mathbf{n}} [0.4 \iiint P_2(\mu'_a \cdot \mu_e) w_{\mathbf{n}}^s(\mu'_a, \mu'_e) g_{\mathbf{n}}(\mu'_a, \mu'_e, 0 | \mu_a, \mu_e, t) d\mu'_a d\mu'_e d\mu_a d\mu_e]. \quad (19)$$

Here we have assumed that all N segments contain an equal number of fluorescent molecules. We also have neglected the rotation of the whole segment and the translational motion of the molecule out of a segment, both very slow processes as compared to the fluorescence lifetime.

Because all the segments are essentially identical with each other, w_n^s or g_n for different n 's are related simply by rotation in space. Therefore, all terms in Eq. 19 become identical after integration. Thus we can choose any particular segment for the calculation of $r(t)$:

$$r(t) = 0.4 \iiint P_2(\mu_a' \cdot \mu_e) w^s(\mu_a', \mu_e') g(\mu_a', \mu_e', 0 | \mu_a, \mu_e, t) d\mu_a' d\mu_e' d\mu_a d\mu_e. \quad (20)$$

Here we have omitted the subscript n , which merely indicates that the probability function is defined within a membrane segment, and does not refer to the whole suspension. For cases *a* and *b*, we obtain similarly

$$r(t) = r_0 \iint P_2(\mu_e' \cdot \mu_e) \hat{w}^s(\mu_e') \hat{g}(\mu_e', 0 | \mu_e, t) d\mu_e' d\mu_e. \quad (21)$$

Eqs. 20 or 21 allow us the calculation of $r(t)$ from a plausible mathematical model of the wobbling motion in the membrane. This theoretical $r(t)$ may in turn be compared with the experimentally obtained $r(t)$.

For example, we may assume that the wobbling motion is described as a diffusion in a potential. If the molecule is symmetric around μ_e , i.e. in case *b*, the master equation will be Smoluchowski's equation (see e.g. ref. 11) of the form

$$\partial \hat{w}(\mu_e, t) / \partial t = \text{div}_{\mu_e} [D_w(\mu_e) \text{grad}_{\mu_e} \hat{w}(\mu_e, t) + \hat{w}(\mu_e, t) f_w(\mu_e)^{-1} \text{grad}_{\mu_e} V(\mu_e)], \quad (22)$$

where the differentiation with μ_e is carried out on a unit sphere, D_w and f_w are the diffusion constant and the frictional coefficient of the wobbling motion, respectively, both of which may depend on the orientation μ_e , and V is the potential. The functions \hat{w}^s and \hat{g} in Eq. 21 are, respectively, the stationary solution and the Green function of the differential Eq. 22. In particular, Einstein's relation $D_w f_w = kT$, where k is the Boltzmann constant and T the absolute temperature, leads to

$$\hat{w}^s(\mu_e) = \text{const} \times \exp [-V(\mu_e)/kT]. \quad (23)$$

For molecules without the symmetry, the master equation will include the differentiation with μ_a , and D_w as well as f_w^{-1} should be regarded as tensors.

THE WOBBLING DIFFUSION CONSTANT AND THE DEGREE OF ORIENTATIONAL CONSTRAINT

In the above, the problem has been the calculation of $r(t)$ from a presumed differential equation. The information we obtain from an experiment, therefore, depends on the choice of a particular mathematical model. However, as we see below, essential information can be extracted directly from an experimental $r(t)$. In showing this, we confine ourselves to cases *a* and *b* for the sake of clear insight. An example of generalization will be given in the next section.

First we let $t \rightarrow \infty$ in Eq. 21. Because $\hat{g}(\mu'_e, 0 | \mu_e, \infty)$ is identical with $\hat{w}^s(\mu_e)$, we obtain

$$r_\infty \equiv r(\infty) = r_0 \iint P_2(\mu'_e \cdot \mu_e) \hat{w}^s(\mu'_e) \hat{w}^s(\mu_e) d\mu'_e d\mu_e. \quad (24)$$

Now we again expand $P_2(\mu'_e \cdot \mu_e)$ as $P_2(\mathbf{n} \cdot \mu'_e) P_2(\mathbf{n} \cdot \mu_e) + \dots$. Since w^s is expected to be symmetric around the normal \mathbf{n} of the membrane, only the first term remains after integration. Thus

$$r_\infty / r_0 = [\int P_2(\mathbf{n} \cdot \mu_e) \hat{w}^s(\mu_e) d\mu_e]^2. \quad (25)$$

This quantity obviously is a measure of the anisotropy of the stationary distribution \hat{w}^s : r_∞ / r_0 is maximal when the emission transition moments μ_e are preferentially aligned along the normal \mathbf{n} ; it becomes null for completely isotropic distribution. Thus it may be termed the degree of orientational constraint. When Eq. 22 applies, r_∞ / r_0 measures the "width" of the potential V in which the molecule wobbles around, as is readily seen from Eq. 23.

Next we consider the region $t \cong 0$. The wobbling diffusion constant may be defined as

$$D_w(\mu'_e) \equiv \lim_{t \rightarrow 0} \frac{1}{4t} \int \omega^2 \hat{g}(\mu'_e, 0 | \mu_e, t) d\mu_e, \quad (26)$$

where ω denotes the angle between μ'_e and μ_e . The integral in the right-hand side is the average of ω^2 at time t . Thus the definition is analogous to the ordinary definition of a rotational diffusion constant. In fact, if the molecule is axially symmetric around μ_e , i.e. in case *b*, $D_w(\mu_e)$ coincides with the rotational diffusion constant around an axis perpendicular to the symmetry axis, and is identical with the one defined in Eq. 22. For a molecule of arbitrary shape, $D_w(\mu_e)$ corresponds to a weighted average of the principal diffusion constants. In any case, D_w may depend on the orientation according to the nature of particular membrane.

For small t , the angle of rotation ω is also small. Therefore, we can use the series expansion

$$P_2(\mu'_e \cdot \mu_e) = \frac{1}{2} (3 \cos^2 \omega - 1) \cong 1 - \frac{3}{2} \omega^2 \quad (27)$$

in Eq. 21. Thus

$$\begin{aligned} r(t) / r_0 &\cong 1 - \frac{3}{2} \iint \omega^2 \hat{w}^s(\mu'_e) \hat{g}(\mu'_e, 0 | \mu_e, t) d\mu'_e d\mu_e \\ &\cong 1 - 6t \int D_w(\mu'_e) \hat{w}^s(\mu'_e) d\mu'_e \\ &\equiv 1 - 6 \langle D_w \rangle t. \end{aligned} \quad (28)$$

Here $\langle D_w \rangle$ is the wobbling diffusion constant averaged over the stationary distribution \hat{w}_s . The value of $\langle D_w \rangle$ can be obtained directly from the initial slope of a measured $r(t)$.

In this way we can infer the dynamical structure of the membrane once $r(t)$ is experimentally determined. The quantity r_∞ / r_0 tells us the degree of confinement of the

orientation of the fluorescent molecule imposed by the structure of the membrane. The initial slope gives us the average "speed" with which the molecule wobbles within the confined angle.

FLUORESCENT PROBES IN LIPID BILAYERS—SIMPLE MODELS

In this section, we proceed into a more detailed discussion based on simplified mathematical models. We concentrate on the system of fluorescent probe molecules dispersed in lipid bilayer membranes. In this system, we expect that the longest axis of the fluorescent molecule is more or less preferentially aligned along the normal of the membrane, i.e. parallel to the long axis of the lipid molecules. As to fluorescent probes, we consider the following three types, which cover a large part of useful probes: i) Rod-shaped molecule with emission transition moment parallel to the long axis. Examples are 1,6-diphenyl-1,3,5-hexatriene (DPH), 2-*p*-toluidinylnaphthalene-6-sulfonate (TNS), etc. ii) Rod-shaped molecule with emission moment perpendicular to the long axis. Examples are 12-(9-anthroyl)stearic acid (AS), *N*-octadecylnaphthyl-2-amino-6-sulfonic acid (ONS), etc. iii) Disk-shaped molecule with both absorption and emission moments in the plane of the disk. Examples are perylene, pyrene, etc.

Rod-Shaped Molecule with Emission Moment Parallel to the Long Axis

Obviously case *b* applies to this type of molecule. Therefore, Eqs. 25 and 28 hold irrespective of r_0 , or of the excitation wavelength. An explicit expression of theoretical $r(t)$ may be obtained by solving Eq. 22, once the wobbling diffusion constant D_w and the potential V are given as functions of the orientation μ_e .

The simplest model will be the following "wobbling-in-cone" model: the orientation μ_e (the long axis) is confined within a cone around the normal \mathbf{n} of the membrane (see Fig. 2) and fluctuates within this cone with a wobbling diffusion constant, D_w ,

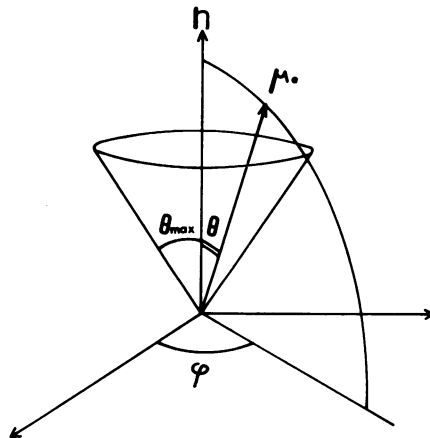


FIGURE 2 Wobbling-in-cone model. The emission transition moment μ_e wobbles around uniformly in the cone.

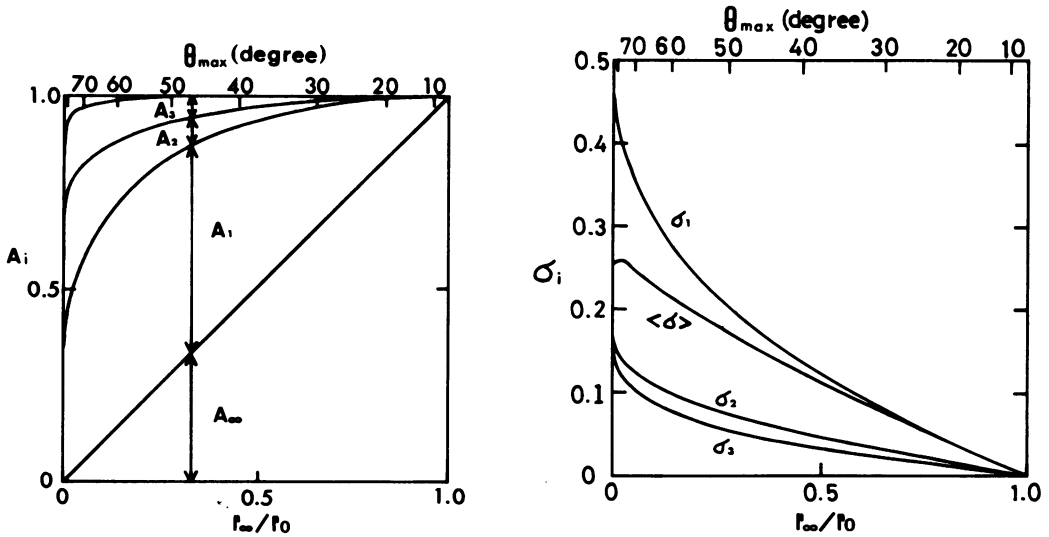


FIGURE 3 Parameters of the wobbling-in-cone model (Eqs. 31 and 33 in text).

which is constant throughout the cone. If we let θ and ϕ be the polar and azimuthal angles of μ_r with respect to \mathbf{n} (Fig. 2), Eq. 22 reduces to

$$\frac{\partial \hat{w}(\theta, \phi, t)}{\partial t} = D_w \left[\frac{1}{\sin \theta} \frac{\partial}{\partial \theta} \left(\sin \theta \frac{\partial}{\partial \theta} \right) + \frac{1}{\sin^2 \theta} \frac{\partial^2}{\partial \phi^2} \right] \hat{w}(\theta, \phi, t), \quad (29)$$

$$(0 \leq \theta \leq \theta_{\max})$$

with the boundary condition

$$\partial \hat{w}(\theta, \phi, t) / \partial \theta = 0 \quad \text{at } \theta = \theta_{\max}. \quad (30)$$

The Green function \hat{g} and the stationary solution \hat{w}^s of the above equation are readily obtained by the method of variable separation.¹ The resultant expression of $r(t)$ is of the form

$$r(t)/r_0 = \sum_{i=1}^{\infty} A_i \exp(-D_w t / \sigma_i), \quad (31)$$

where A_i and σ_i are constants which depend only on θ_{\max} . In particular, the stationary term A_{∞} , which corresponds to $\sigma_{\infty} = \infty$, is given by

$$A_{\infty} = r_{\infty}/r_0 = [\frac{1}{2} \cos \theta_{\max} (1 + \cos \theta_{\max})]^2. \quad (32)$$

Values of several other constants are shown in Fig. 3.

¹ $\hat{g}(\theta', \phi', 0 | \theta, \phi, t) = \sum_{\nu, m} P_{\nu}^{-m}(\cos \theta') P_{\nu}^m(\cos \theta) \exp im(\phi - \phi') \exp[-\nu(\nu + 1)D_w t]$, where P_{ν}^m are Legendre's associated functions which satisfy the boundary condition 30, and $\hat{w}^s(\theta, \phi) = 1/2\pi(1 - \cos \theta_{\max})$.

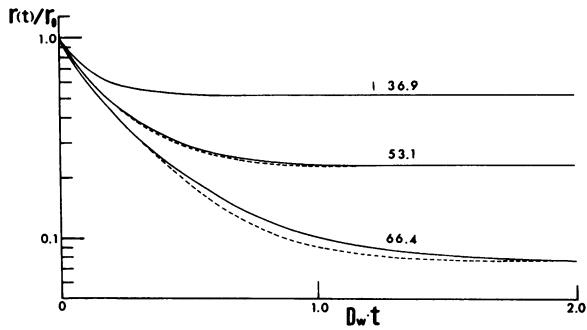


FIGURE 4 Theoretical curves of fluorescence anisotropy decay for the wobbling-in-cone model. The curves from top to bottom correspond to cone angles θ_{\max} of 36.9°, 53.1°, and 66.4°. Dashed lines are approximate expressions given by Eq. 33. D_w is the wobbling diffusion constant.

Examples of the curve $r(t)/r_0$ are illustrated in Fig. 4. In all cases the initial slope is equal to $6D_w$, as is expected from Eq. 28. In the figure, the broken lines represent an approximate expression

$$r(t)/r_0 = A_\infty + (1 - A_\infty) \exp(-D_w t / \langle \sigma \rangle), \quad (33)$$

where

$$\langle \sigma \rangle = \sum_{i \neq \infty} A_i \sigma_i. \quad (34)$$

The simple expression 33 is a good approximation to the theoretical $r(t)/r_0$ of the wobbling-in-cone model. The quantity $\langle \sigma \rangle / D_w$ is the time with which the initially photoselected distribution of orientations approaches the stationary distribution. As is seen in Fig. 3b, this apparent relaxation time is roughly proportional to $(r_0 - r_\infty)/r_0$. Naturally, the relaxation is slower for the wider cone.

Rod-Shaped Molecule with Emission Moment Perpendicular to the Long Axis

In this case, the stationary distribution of emission moment μ_e is expected to be maximal in the plane of the membrane. The principal mode of motion of μ_e will be "spinning" around the long axis of the molecule, on which the effect of wobbling motion of the long axis is superposed. Eqs. 25 and 28 as well as the following apply only to the case where $r_0 \cong 0.4$.

A simple model for this type of molecules is the one in which the stationary distribution of μ_e is uniform over the equatorial band $\theta_{\min} \leq \theta \leq \pi - \theta_{\min}$, i.e. the outside of the cone shown in Fig. 2 (θ_{\max} in the figure should, in this case, read θ_{\min}). For this model, Eq. 25 becomes

$$r_\infty/r_0 = [\frac{1}{2}(1 - \cos^2 \theta_{\min})]^2. \quad (35)$$

In general, the rotational diffusion constant of this molecule around the axis perpendicular to the long axis is different from the one corresponding to spinning around

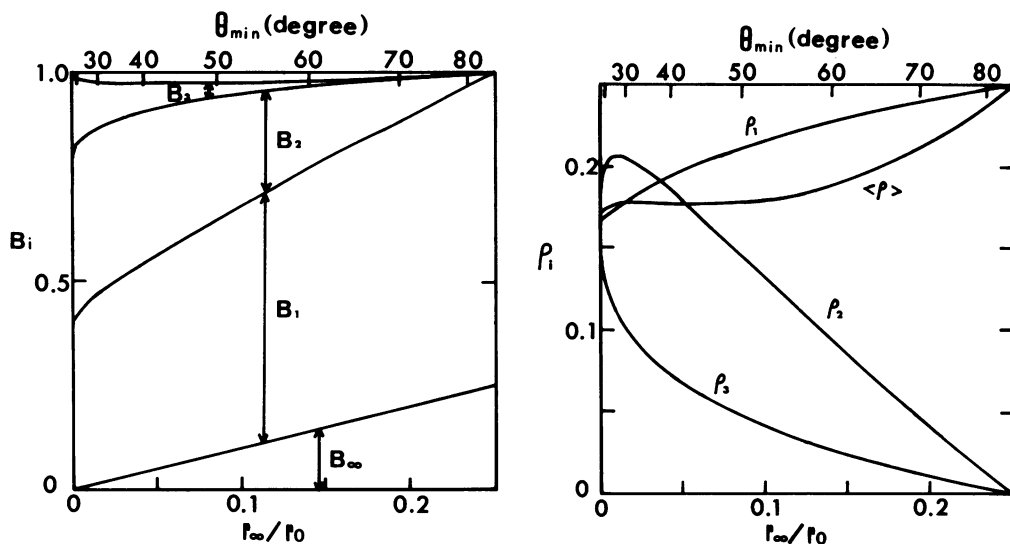


FIGURE 5 Parameters of the spinning-in-equatorial-band model (Eqs. 36 and 37 in text).

the long axis. If, in the above model, we further simplify the situation to equate both diffusion constants to D_s , the spinning diffusion constant, the simple diffusion equation of the form 29 holds in the region $\theta_{\min} \leq \theta \leq \pi - \theta_{\min}$. This rather rough approximation is vindicated to some extent for molecules like AS or ONS whose backbone is considered flexible.

Under the above assumption, the theoretical expression of $r(t)$ is again of the form

$$r(t)/r_0 = \sum_{i=1}^{\infty} B_i \exp(-D_s t/\rho_i), \quad (36)$$

where B_{∞} is equal to r_{∞}/r_0 in Eq. 35, $\rho_{\infty} = \infty$. Other values can be read from Fig. 5. Typical theoretical curves are given in Fig. 6. In this case, too, the initial slopes are equal to $6D_s$, and the curves can be approximated by an expression (broken lines)

$$r(t)/r_0 = B_{\infty} + (1 - B_{\infty}) \exp(-D_s t/\langle \rho \rangle). \quad (37)$$

Note that as far as the rotation around the long axis is free, the value of r_{∞}/r_0 does not exceed 0.25.

Disk-Shaped Molecule

As Weber (12) has pointed out, both the absorption and emission moments of aromatic molecules are generally contained in the plane of the aromatic rings. In this subsection, we consider those aromatic molecules whose shape is approximated by a disk. The most probable orientation of these molecules in the lipid bilayer will be the one in which the axis perpendicular to the plane of the disk is contained in the plane of the membrane. The molecule will rotate principally in the plane of the disk (in-plane rotation), whereas the out-of-plane motion tends to be more or less restricted.

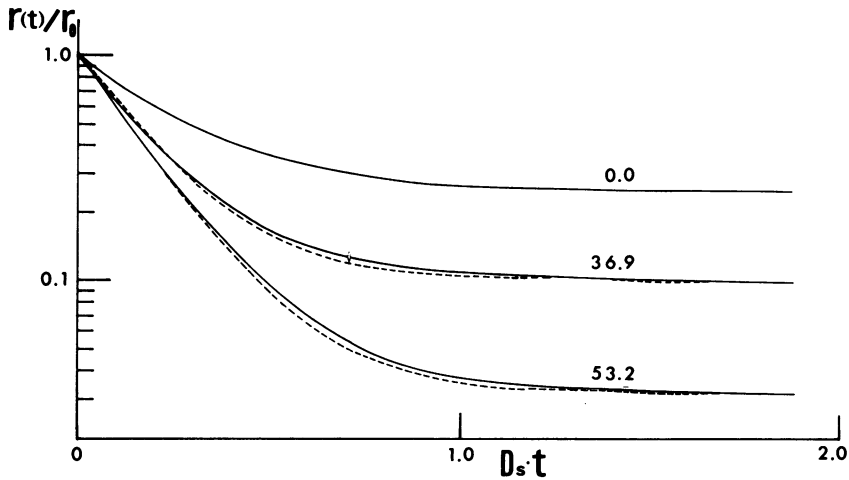


FIGURE 6 Theoretical curves of fluorescence anisotropy decay for the spinning-in-equatorial-band model. The curves from top to bottom correspond to $\theta'_{\max} \equiv \pi/2 - \theta_{\min}$ of 0.0° , 36.9° , and 53.2° . Dashed lines are approximate expressions given by Eq. 37. D_s is the spinning diffusion constant.

In the following, we extend the discussion of r_∞/r_0 and $\langle D_w \rangle$ given in the preceding section, which has been useful primarily for rodlike molecules. First we let $t \rightarrow \infty$ in Eq. 20 and proceed in the way in which we obtained Eq. 25. We obtain

$$r_\infty = 0.4 \left[\iint P_2(\mathbf{n} \cdot \boldsymbol{\mu}'_a) w^s(\boldsymbol{\mu}'_a, \boldsymbol{\mu}'_e) d\boldsymbol{\mu}'_a d\boldsymbol{\mu}'_e \right] \left[\iint P_2(\mathbf{n} \cdot \boldsymbol{\mu}_e) w^s(\boldsymbol{\mu}_a, \boldsymbol{\mu}_e) d\boldsymbol{\mu}_a d\boldsymbol{\mu}_e \right], \quad (38)$$

a generalization of Eq. 25. For disklike molecules, in particular, the two integrations in the above equation should give the same value. Hence

$$r_\infty/0.4 = \left[\int P_2(\mathbf{n} \cdot \boldsymbol{\mu}_e) \hat{w}^s(\boldsymbol{\mu}_e) d\boldsymbol{\mu}_e \right]^2. \quad (39)$$

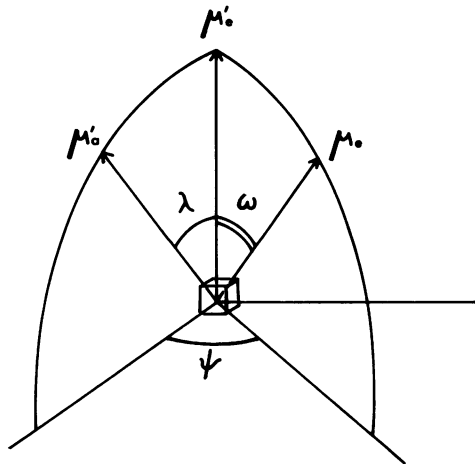


FIGURE 7 Definition of angles in Eq. 40.

Note the difference between Eqs. 25 and 39. For disklike molecules, r_∞ is independent of r_0 or of the excitation wavelength. If the out-of-plane motion is completely restricted, r_∞ is equal to 0.1.

Next we consider the region $t \cong 0$, starting from the general expression 20. Let D_i and D_o be the rotational diffusion constants corresponding to the in-plane and the out-of-plane motion, respectively. Then for $t \cong 0$,

$$\int g(\mu'_a, \mu'_c, 0 | \mu_a, \mu_c, t) d\mu_a \cong \frac{1}{4\pi\sqrt{D_i D_o t}} \exp \left[-\frac{\omega^2 \cos^2 \psi}{4D_i t} - \frac{\omega^2 \sin^2 \psi}{4D_o t} \right], \quad (40)$$

where ω and ψ are defined in Fig. 7. We again use expansion 14, which for small ω becomes

$$P_2(\mu'_a \cdot \mu_c) \cong P_2(\cos \lambda)(1 - \frac{3}{2}\omega^2) + P_2(\cos \lambda)\omega \cos \psi + \frac{1}{4}P_2(\cos \lambda)\omega^2 \cos 2\psi. \quad (41)$$

Substituting Eqs. 40 and 41 into 20, we obtain

$$r(t)/r_0 \cong \begin{cases} 1 - 6 \langle \frac{D_i + D_o}{2} \rangle t & \text{for } \lambda = 0 \quad (r_0 = 0.4) \\ 1 - 6 \langle D_o \rangle t & \text{for } \lambda = \pi/4 \quad (r_0 = 0.1) \\ 1 - 6 \langle D_i \rangle t & \text{for } \lambda = \pi/2 \quad (r_0 = -0.2) \end{cases} \quad (42)$$

where $\langle \rangle$ denotes the average over possible dependence of D_i and D_o on the orientation in the stationary distribution w^s . Thus we can measure both the diffusion constants by varying λ , which is the function of the excitation wavelength. The fact that we can discriminate D_i and D_o by suitable selection of the excitation wavelength has been pointed out by Shinitzky et al. (13) for the case of stationary excitation. Note that Eq. 42 is valid even in an anisotropic environment like membrane, because the "diffusion" term dominates over the "potential" term at $t \cong 0$.

For a disklike molecule interposed in the array of rodlike lipid molecules, the stationary distribution of μ_c may be approximated as uniform over a meridian band instead of the equatorial band discussed under Rod-shaped molecules (a complete out-of-plane turn will take a much longer time than the in-plane rotation or the out-of-plane wobbling). When the difference between D_i and D_o is small, the mode of rotational motion is exactly the same as in rod-shaped molecules, except that the symmetry axis is contained in the plane of the membrane instead of coinciding with the normal. Under these assumptions, therefore, theoretical $r(t)$ is given by the same expression as Eq. 36, which is valid for $r_0 \cong 0.4$.

APPLICATION TO EXPERIMENTAL DATA

The theory combined with a suitable experimental technique will enable us to visualize the wobbling motions in membranes. This section briefly discusses the experimental aspect; the next section illustrates an example.

In its general form the theory describes the motion of a fluorophore by two parameters, the (average) wobbling diffusion constant $\langle D_w \rangle$ and the degree of orienta-

tional constraint r_∞/r_0 . Since $\langle D_w \rangle$ and r_∞/r_0 are determined from the initial slope and the stationary value of an experimental $r(t)$, the measuring system must have a good time resolution as well as a wide dynamic range. The latter is required because the total fluorescence intensity decays substantially by the time $r(t)$ reaches the stationary value. These requirements are met by a pulse fluorometer employing the single photon counting technique (1,2). An apparatus specifically designed for the present purpose has been described elsewhere (7).

With currently used pulse fluorometers, a precise $r(t)$ is obtained only through a deconvolution procedure that corrects the observed data for the time characteristics of the apparatus. The ordinary procedure is to assume that $r(t)$ is expressed as a sum of several exponentials:

$$r(t) = \sum_{i=1}^N r_i \exp(-t/\chi_i), \quad (43)$$

and determine the values of r_i and χ_i by curve fitting (7) or by one of the alternative methods (1,2). When the environment of fluorophores is anisotropic, one of the exponential terms becomes a constant ($\chi_N = \infty$, $r_N = r_\infty$), from which the degree of orientational constraint is obtained. The wobbling diffusion constant is given by

$$\langle D_w \rangle = \left[\sum_{i=1}^{N-1} r_i/\chi_i \right] / 6 \sum_{i=1}^N r_i. \quad (44)$$

Often the mode of wobbling motion may be inferred from available knowledge. In this case, the corresponding differential equation (such as Eqs. 22 or 29) is first solved to construct a theoretical $r(t)$. Then parameters in the theoretical $r(t)$ are determined by deconvolution (curve fitting) using this theoretical $r(t)$ instead of Eq. 43. In the simple models in the previous section, in particular, all theoretical $r(t)$ s have the approximate form:

$$r(t) = (r_0 - r_\infty) \exp(-t/\chi) + r_\infty. \quad (45)$$

Therefore, the ordinary deconvolution procedure can be used to determine r_0 , r_∞ , and χ . Then, D_w and θ_{\max} in the wobbling-in-cone model, for example, are obtained from Eq. 32 and the relation:

$$D_w = \langle \sigma \rangle / \chi, \quad (46)$$

where the value of $\langle \sigma \rangle$ is read from Fig. 3b.

DYNAMIC STRUCTURE OF LIPID BILAYERS AS REVEALED BY THE MEASUREMENT OF FLUORESCENCE POLARIZATION DECAY

The motion of a fluorescent probe 1,6-diphenyl-1,3,5-hexatriene (DPH) in liposomes of dipalmitoylphosphatidylcholine (DPPC) has already been analyzed by the theory. Since the details have been reported elsewhere (8), only an outline is given here.

DPH is a probe for the hydrocarbon region of lipid bilayers; it is a rod-shaped molecule with μ_a and μ_e lying parallel to the long axis (14). Thus, it belongs to the class *i* molecules discussed in the section of simple models. DPPC bilayers in aqueous dispersion undergo the gel-to-liquid-crystalline phase transition at about 40°C (15). Fluorescence polarization decay measurements (8) showed that $r(t)$ of DPH in DPPC bilayers closely follows Eq. 45 both below and above the phase transition temperature. Finite values of r_∞ clearly indicated an anisotropic environment for the DPH molecules, in agreement with the observation (16) that DPH in lipid bilayers are preferentially oriented along the normal of the membrane.

The motion of the DPH molecules was analyzed by the wobbling-in-cone model as outlined in the previous section. The cone angle θ_{\max} showed a sigmoidal dependence on temperature: θ_{\max} was about 20° at low temperatures and abruptly increased to about 70° at the phase transition. In contrast to θ_{\max} , the wobbling diffusion constant D_w did not show a discontinuity at the transition; D_w increased roughly exponentially with temperature from 0.04 ns⁻¹ at 5°C to 0.3 ns⁻¹ at 60°C.

Since the thickness of the rod-shaped DPH approximates that of the hydrocarbon chain of a lipid molecule, each probe molecule presumably replaces one acyl chain in the bilayer structure. Tumbling of the DPH rod occurs as a neighboring acyl chain(s) wobbles out of the cone. Thus, the motion of DPH directly reflects the thermal motion of lipid acyl chains. The data suggest a considerable fluctuation of the chains even in the gel state; above the transition, the interior of bilayers becomes highly disordered, as shown by the large cone angle, but still retains the orientational anisotropy. The continuous change of D_w across the transition temperature suggests that the frequency of fluctuation of acyl chains is not much affected by the phase transition.

“Viscosity in the cone” may be estimated from the wobbling diffusion constant and the effective volume of the DPH molecule. Values thus obtained were an order of magnitude smaller than the “microviscosity” values estimated from steady-state fluorescence polarization measurements (14,17). The discrepancy arises because the microviscosity does not discriminate the dynamic friction (reflected by D_w) and the static orientational constraint. An isotropic medium is adequately characterized by a single parameter such as the microviscosity, whereas description of an anisotropic structure such as membrane requires at least two parameters, e.g. the wobbling diffusion constant and the degree of orientational constraint, or the viscosity in the cone and the cone angle.

CONCLUSION

By the nanosecond fluorescence polarization technique, we can obtain information about molecular motions within, and restricted by, a structure. The wobbling motion in membranes is an example. Others are the internal motion of a residue or a subunit within a macromolecule, the flexing motion in a fibrous structure, etc. Generally, the motion is wobbling rather than free rotation, because a particular orientation(s) of the mobile unit is favored by the surrounding structure.

Although the discussion in the foregoing sections has been focused on membrane systems, most of the results obtained there are applicable to other systems as well: no assumptions peculiar to membrane have been made. Since measurements are usually made on suspensions, Eqs. 20 or 21 afford the basis of analysis for all systems. These equations correlate the polarization decay in a general way with the wobbling motion in the structure, provided the rotation of the whole structure is slow as compared to the internal motions. The simplest and yet fully informative way of analysis is to describe the wobbling motion in terms of the wobbling diffusion constant and the degree of orientational constraint. When the mode of the wobbling is known or can be inferred, the analysis using one of the simple models offers a clearer picture.

In this regard, a comment should be made on the symbol \mathbf{n} , introduced as the normal of a membrane segment. It should, in general, be understood as the average direction of the emission transition moment. In other words, \mathbf{n} corresponds to the (approximate) symmetry axis of the local structure in which the unit containing the fluorophore wobbles.²

When the concentration of fluorophores in the structure is high, the excitation energy transfer between fluorophores (19) also contributes to the depolarization of fluorescence. Formally, Eqs. 20 and 21 can include this situation. Consider an example where membrane contains a dense population of relatively immobile fluorophores. Then the evolution function represents the probability of energy transfer that results in the assigned change of the orientation of emission transition moment. The initial slope of the curve $r(t)/r_0$ is roughly proportional to the average rate of energy transfer, which in turn will be proportional to the third power of the number of fluorophores per unit area if the transfer is of the Förster type (19). The quantity r_∞/r_0 may still be called the degree of orientational constraint: it represents the degree of parallelism among the orientation of fluorophores in the membrane. Note that, in this case, \mathbf{n} in Eq. 25 should be read the direction of the emission moment averaged over all the interacting fluorophores; whereas in case of the wobbling motion it corresponds to the direction of the moment in an individual fluorophore averaged over time.

Recently a new method has been developed to follow rotational or wobbling motion through the measurement of transient absorption dichroism of triplet probes (20). This method covers a time range of microseconds and milliseconds. Because the fluorescence polarization technique is useful in the nanosecond region, both methods complement each other. In the study of biomembranes, fluorescent polarization is suitable to probe the motion of lipids while the transient dichroism method will be powerful for protein wobbling. The theory developed here is directly applicable to this new technique, because both methods observe essentially the same quantity, the anisotropy of the orientational distribution of transition moments.

²Even in lipid bilayers, the long axis of lipid molecules is usually inclined from the normal of the membrane at temperatures below the phase transition (18). In this case, of course, \mathbf{n} should be taken parallel to the long axis.

Numerical calculations in this work were done by Dr. M. I. Kanehisa, to whom the authors are grateful.

Received for publication 4 March 1977 and in revised form 9 August 1977.

REFERENCES

1. WAHL, P. 1975. Nanosecond pulsefluorimetry. *New Tech. Biophys. Cell Biol.* **2**:233.
2. YGUERABIDE, J. 1972. Nanosecond fluorescence spectroscopy of macromolecules. *Methods Enzymol.* **26**:498.
3. KINOSITA, K. JR., S. MITAKU, and A. IKEGAMI. 1975. Degree of dissociation of apohemoglobin studied by nanosecond fluorescence-polarization technique. *Biochim. Biophys. Acta.* **393**:10.
4. YGUERABIDE, J., H. F. EPSTEIN, and L. STRYER. 1970. Segmental flexibility in an antibody molecule. *J. Mol. Biol.* **51**:573.
5. WAHL, P., M. KASAI, and J. P. CHANGEUX. 1971. A study on the motion of proteins in excitable membrane fragments by nanosecond fluorescence polarization spectroscopy. *Eur. J. Biochem.* **18**:332.
6. CHEN, L. A., R. E. DALE, S. ROTH, and L. BRAND. 1977. Nanosecond time-dependent fluorescence depolarization of diphenylhexatriene in dimyristoyllecithin vesicles and the determination of "microviscosity." *J. Biol. Chem.* **252**:2163.
7. KINOSITA, K. JR., S. MITAKU, A. IKEGAMI, N. OHBO, and T. L. KUNII. 1976. Construction of a nanosecond fluorometric system for applications to biological samples at cell or tissue levels. *Jpn. J. Appl. Phys.* **15**:2433.
8. KAWATO, S., K. KINOSITA, JR., and A. IKEGAMI. 1977. Dynamic structure of lipid bilayers studied by nanosecond fluorescence techniques. *Biochemistry.* **16**:2319.
9. TAO, T. 1969. Time-dependent fluorescence depolarization and Brownian rotational diffusion coefficients of macromolecules. *Biopolymers.* **8**:609.
10. BELFORD, G. G., R. L. BELFORD, and G. WEBER. 1972. Dynamics of fluorescence polarization in macromolecules. *Proc. Natl. Acad. Sci. U.S.A.* **69**:1392.
11. CHANDRASEKHAR, S. 1943. Stochastic problems in physics and astronomy. *Rev. Mod. Phys.* **15**:1.
12. WEBER, G. 1973. Polarized fluorescence. In *Fluorescence Techniques in Cell Biology*. A. A. Thayer and M. Sernetz, editors. Springer-Verlag KG, Berlin, W. Germany. 5.
13. SHINITZKY, M., A. C. DIANOUX, C. GITLER, and G. WEBER. 1971. Microviscosity and order in the hydrocarbon region of micelles and membranes determined with fluorescent probes. I. Synthetic micelles. *Biochemistry.* **10**:2106.
14. SHINITZKY, M., and Y. BARENHOLZ. 1974. Dynamics of the hydrocarbon layer in liposomes of lecithin and sphingomyelin containing dicetylphosphate. *J. Biol. Chem.* **249**:2652.
15. CHAPMAN, D. 1975. Phase transitions and fluidity characteristics of lipids and cell membranes. *Q. Rev. Biophys.* **8**:185.
16. ANDRICH, M. P., and J. M. VANDERKOOI. 1976. Temperature dependence of 1,6-diphenyl-1,3,5-hexatriene fluorescence in phospholipid artificial membranes. *Biochemistry.* **15**:1257.
17. LENTZ, B. R., Y. BARENHOLZ, and T. E. THOMPSON. 1976. Fluorescence depolarization studies of phase transitions and fluidity in phospholipid bilayers. 1. Single component phosphatidylcholine liposomes. *Biochemistry.* **15**:4521.
18. TARDIEU, A., V. LUZZATI, and F. C. REMAN. 1973. Structure and polymorphism of the hydrocarbon chains of lipids: a study of lecithin-water phases. *J. Mol. Biol.* **75**:711.
19. FÖRSTER, T. 1965. Delocalized excitation and excitation transfer. In *Modern Quantum Chemistry*. O. Sinanoglu, editor. Academic Press, Inc., New York. 93.
20. CHERRY, R. J., A. BÜRKL, M. BUSSLINGER, G. SCHNEIDER, and G. R. PARISH. 1976. Rotational diffusion of band 3 proteins in the human erythrocyte membrane. *Nature (Lond.)* **263**:389.